JOURNAL OF APPLIED ELECTROCHEMISTRY 17 (1987) 997-1001

Mono- and multilayer formation studies of silver iodide on silver electrode from iodide-containing solutions

S. JAYA, T. PRASADA RAO*, G. PRABHAKARA RAO

Central Electrochemical Research Institute, Karaikudi 623 006, India

Received 20 August 1986; revised 2 January 1987

Cyclic voltammetric and single potential step current–time experiments were carried out on the silver electrode in order to understand the nature of kinetic processes involved during the mono- and multilayer formation of silver iodide. Two pre-peaks were noticed at potentials more negative to the multilayer formation and to the Ag/AgI reversible potential. These pre-peaks were found to arise during the monolayer formation of AgI via the adsorption–desorption processes. On the other hand, the multilayer formation of AgI processes occurs by instantaneous nucleation–growth.

1. Introduction

Several electrochemical properties of insoluble metal halides have been studied in the past and interest in silver iodide, in particular, has risen from its use as an ion-specific electrode [1] and as a model system in studies of the stability of lyophobic colloids [2].

As an ion-selective electrode the Ag/AgI electrode has been used in the detection and determination of silver, iodide and other ions such as cyanide and mercury [3]. The electrode can function as either one of the second kind (composed of an AgI film on silver substrate) or as a solid state AgI membrane electrode. In the model studies of the stability of lyophobic colloids most of the work was directed towards the thermodynamics and only to a very modest extent to the kinetic aspects of stability phenomena [4]. Much work has also been carried out with regard to the film formation between silver and iodide [5] as well as other anions [6–9]. To date there have been no reports in the literature of the electrochemical phase formation (ECPF) of monolayers of metal iodides on metal electrodes in aqueous solution, though the formation of metal iodide monolayers should be as likely as the metal oxide monolayers.

In this paper we present an analysis of cyclic voltammetric and potentiostatic current–time transient studies conducted to elucidate the mono- and multilayer formation of silver iodide.

2. Experimental details

Cyclic potentiodynamic and potentiostatic experiments were carried out with polycrystalline silver electrodes (Johnson Mathey, 99.999%, 7 mm in diameter), pressure-fitted in a Teflon holder and set in with Araldite. The reference electrode used was a normal calomel (1 M KCl) electrode (NCE) and all potentials were referred to this. A Luggin probe was positioned ~ 1 mm from the electrode surface. Under these conditions, the maximum deviation from the programmed potential due to electrolyte resistance was $\leqslant 50$ mV. The potential of the working electrode was controlled by a Wenking potentiostat (Model LB 75 M) with a response time of $\sim 1\,\mu$s fed by a voltage scan generator (Model VSG 72) supplying current to a platinum counter electrode of area $\sim 6\,\text{cm}^2$. Electrolytes were made from analytical grade reagents and triply distilled water (distilled in an all-quartz triple distillation unit). A Ricadenki xy/t recorder with pen speeds of $> 120\,\text{cm}\,\text{s}^{-1}$ was used for recording current–potential and current–time profiles in cyclic voltammetric and potential step experiments, respectively. Experiments were conducted at 303 K and deaeration was

* To whom correspondence should be addressed.

0021–891X/87 $03.00 + .12

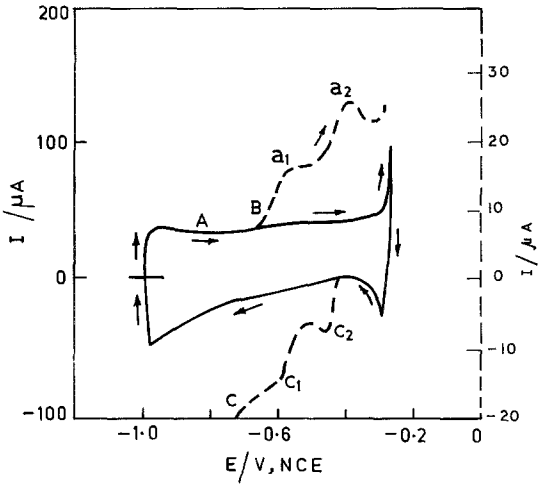

Fig. 1. Cyclic voltammogram obtained with polycrystalline silver disc electrode in 0.01 M KI containing 0.1 M $NaNO_3$ as supporting electrolyte in the potential scan range -1.0 to -0.25 V vs NCE at a sweep rate of 180 mV s^{-1}. Curve A is drawn at 25 μA cm^{-1} while curves B and C are drawn at 5 μA cm^{-1} on current scale.

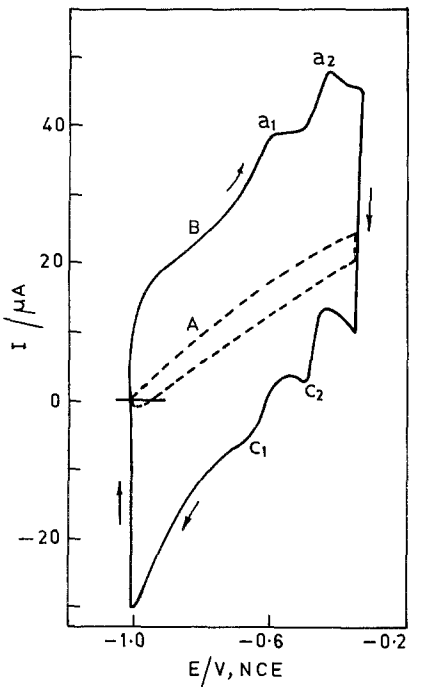

Fig. 2. Cyclic voltammograms obtained with polycrystalline silver disc electrode in 0.1 M $NaNO_3$ (curve A) and 0.01 M KI in 0.1 M $NaNO_3$ (curve B) in the potential scan range -1.0 to -0.34 V vs NCE at a sweep rate of 180 mV s^{-1}.

achieved by bubbling pure N_2 through the electrolyte.

3. Results and discussion

3.1. *Monolayer formation studies*

3.1.1. Cyclic voltammetric studies. Fig. 1, curve A, shows the cyclic voltammogram of a polycrystalline silver disc electrode in a quiscent solution of 0.01 M potassium iodide at 0.1 M $NaNO_3$. There is a sudden rise of current at -0.28 V vs NCE, presumably due to the formation of an AgI phase [5]. When the potential scan is reversed in the initial stages of AgI multilayer formation, surface growth loops are conspicuously absent indicating that AgI phase formation does not occur by 3-d nucleation and subsequent grain growth [10]. Curves B and C of Fig. 1, obtained by recording the cyclic voltammogram on a much more sensitive current scale, shows the presence of two pre-peaks before the multilayer formation of AgI at -0.61 and -0.45 V (a_1 and a_2) and their corresponding reduction peaks at -0.65 and -0.48 V (c_1 and c_2). The currents associated with the pre-peaks are much smaller than that for the main anodic and cathodic peaks for AgI multilayer formation, and subsequent reduction indicates that a much smaller amount of anodic film is formed in the pre-peak region.

In the study of pre-peaks, each experiment was commenced by cycling the potential of the silver disc electrode in 0.1 M $NaNO_3$ (Fig. 2, curve A). In the potential range studied, only charging current was observed. However, on addition of 0.01 M KI, the anodic pre-peaks (a_1 and a_2) and cathodic counterparts (c_1 and c_2) developed immediately (Fig. 2, curve B). The size and shape of the pre-peaks were found to be stable with time of potential cycling which clearly indicates that the pre-peaks cannot be related to the presence of impurities in the solution, which are expected to build up with time on the electrode surface. Further, the pre-peaks remained stable and unchanged despite extending the potential scan limits negative to the hydrogen evolution or positive to the multilayer formation of AgI (Fig. 3). When the potential scan was extended to still more positive potentials, much more AgI film formation occurred and the reduction of AgI pre-peak was obliterated by the

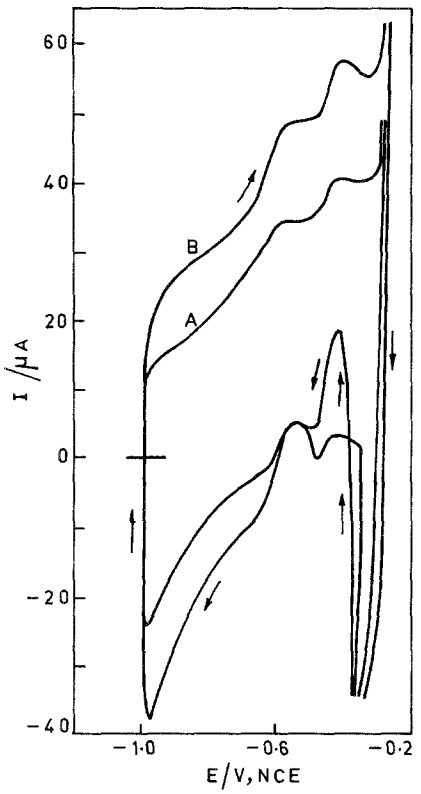

Fig. 3. Cyclic voltammograms obtained with polycrystalline silver disc electrode in 0.01 M KI containing 0.1 M $NaNO_3$ as supporting electrolyte in the potential scan range -1.0 to -0.260 V vs NCE at sweep rates of 180 (curve A) and 270 mV s^{-1} (curve B).

large cathodic peak of AgI reduction. With larger amounts of AgI multilayer formation, the surface area of the electrode began to increase with each complete cycle of potential scan and the magnitude of the pre-peak was also seen to increase with increasing electrode area.

The plot of peak current (I_p) versus sweep rate (v) gives linear plots for all the pre-peaks, namely a_1, a_2, c_1 and c_2 (curves A, B, C and D of Fig. 4, respectively) indicating that the AgI formation is a surface reaction, i.e. involving the monolayer formation of AgI. This is further confirmed by the fact that the total charge transferred for peaks a_1 and a_2 is 3.7 μC, which is well below the charge expected for a full monolayer coverage, and also that the peak potentials of a_1 and a_2 are more negative to the Ag/AgI reversible potential, namely -0.315 V vs NCE [11].

The monolayer peaks thus identified were subjected to analysis according to the theoretical

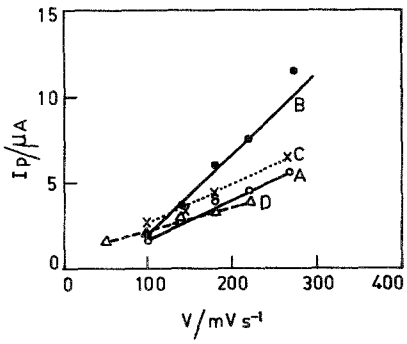

Fig. 4. Plots of peak currents (I_p) of a_1, a_2, c_1 and c_2 (curves A, B, C and D, respectively) with sweep rate.

models suggested by Bosco and Rangarajan [12] to elucidate the kinetic processes involved during their formation. The effect of sweep rate on peak width at half-height ($E_{p_{1/2}}$) of the four monolayer peaks is shown in Table I. From the table it is clear that the $E_{p_{1/2}}$ values at higher sweep rates are $\geqslant 90$ mV, which rules out the possibility of monolayer formation of AgI by instantaneous or progressive nucleation–growth-controlled processes. This is further confirmed by the absence of linearity for I_p versus E_p, I_p versus $1/E_p^2$ and I_p versus coth E_p (where I_p and E_p are non-dimensional quantities) [12]. Further, $E_{p_{1/2}}$ values are 120 mV for a_1 and c_1 and 90 mV for a_2 and c_2, indicating that monolayer formation occurs by adsorption kinetics. A detailed account of the study of various kinetic parameters for adsorption controlled processes are discussed by Angerstein-Kozlowska *et al.* [13] and Laviron [4].

For the monolayer peaks a_1, c_1 and c_2 the peak

Table 1. Effect of sweep rate on peak width at half-height

Sweep rate (v, *mV* s^{-1})	*Peak width at half-height* ($E_{p_{1/2}}$, *mV*)			
	a_1	a_2	c_1	c_2
18	120	90	120	90
22	120	90	120	80
30	125	90	120	85
50	120	90	110	90
100	120	90	110	90
140	120	95	125	90
180	120	90	120	90
220	125	90	125	95
270	125	90	120	90
400	125	90	125	90

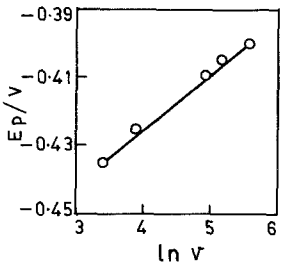

Fig. 5. Plot of peak potential (E_p) versus ln v for peak a_2.

potential (E_p) values remain unaltered in the sweep rate range studied, indicating the reversibility of these processes. On the other hand for the monolayer peak a_2, the E_p value remains constant at sweep rates $\leqslant 30\,mV\,s^{-1}$. At sweep rates $> 30\,mV\,s^{-1}$ the E_p values shift to more positive potentials. Hence, the processes responsible for peak a_2 are reversible only at lower sweep rates ($\leqslant 30\,mV\,s^{-1}$) and become irreversible at higher sweep rates ($> 30\,mV\,s^{-1}$). Fig. 5 shows the linear plot of E_p versus ln v for peak a_2 as expected for an irreversible process at higher sweep rates. Over the whole range of sweep rates studied, including the slowest sweep rate, a_1 and c_1 and a_2 and c_2 were not symmetrical with respect to the potential axis, indicating that the overall monolayer formation and its dissolution processes are irreversible. Further, ΔE_p (difference between E_p values of a_1 and c_1) increases with $1/m$ as seen from Fig. 6, where m is given by

$$\frac{RT}{F}\left(\frac{k_s}{nv}\right)$$

where k_s is the heterogeneous rate constant.

From the ΔE_p values for peak a_1 and c_1 and

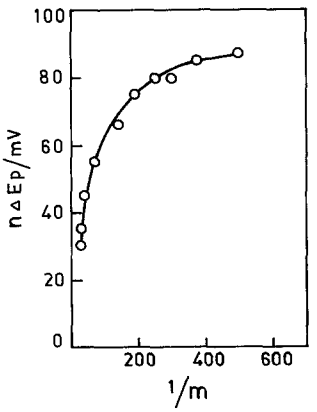

Fig. 6. Plot of ΔE_p versus $1/m$.

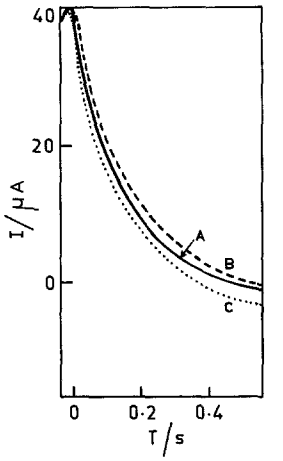

Fig. 7. Potentiostatic current–time transients during monolayer formation of AgI from 0.01 M KI in aqueous 0.1 M $NaNO_3$ by potentiostating the silver electrode at -0.58 (curve A), -0.55 (curve B) and -0.50 V vs NCE (curve C).

a_2 and c_2, when $v_a = v_c = 0.1$ V, the k_s values were calculated to be 22.0 and $35.49\,s^{-1}$. The $E_{p_{1/2}}$ values for a_1 and c_1 (at higher sweep rates) are 125 mV and by equating this with $62.5/\alpha n$, the charge transfer coefficient (α) value was calculated to be 0.5 with $n = 1$.

3.1.2. Current–time transient studies. Figs 7 and 8 show some examples of current–time transients obtained by potentiostating the silver electrode at potentials in the region corresponding to peaks a_1 and a_2, respectively. A rapidly falling current–time transient with no maxima or minima at lower or higher times indicates the absence of

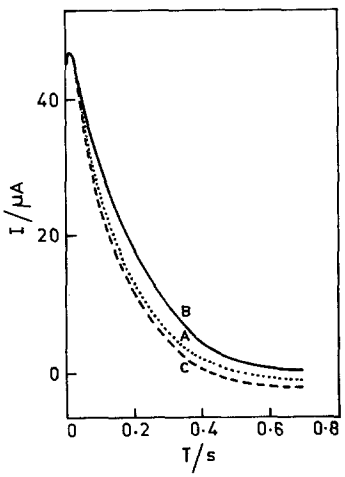

Fig. 8. Same as in Fig. 7 but by potentiostating at -0.41, -0.38 and -0.32 V vs NCE (curves A, B and C respectively).

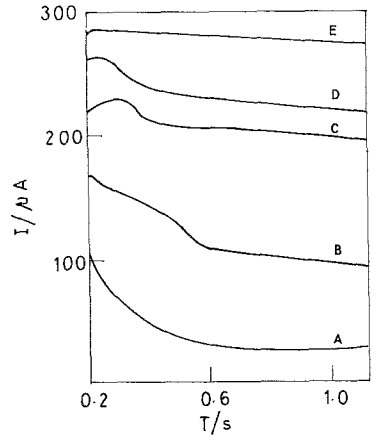

Fig. 9. Potentiostatic current–time transients for the electrodeposition of AgI on silver from 0.1 M KI in aqueous 0.1 M $NaNO_3$ solution by potentiostating at overpotentials of 0, 2, 13.5, 15 and 28 mV (curves A, B, C, D and E, respectively).

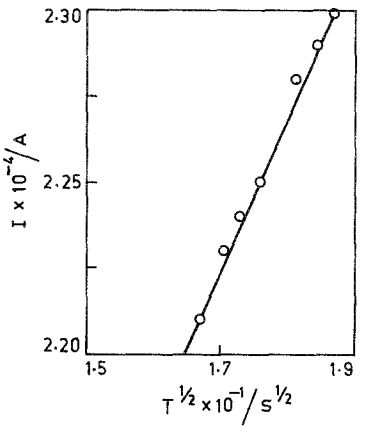

Fig. 10. Linear dependence between current and $T^{1/2}$ for the middle and rising section of transient (Fig. 9, curve C).

nucleation–growth processes and confirms that the monolayer formation occurs by adsorption–desorption processes as concluded in the voltammetric studies.

3.2. *Multilayer formation studies*

Cyclic voltammetric studies were described by Birss and Wright [5] in their recent communication regarding the multilayer formation of silver iodide. Hence, the multilayer formation of silver iodide on polycrystalline silver electrodes was studied only by current–time transient studies.

3.2.1. Current–time transient studies. Single-step potentiostatic current–time (I–T) transients were obtained at various potentials and some are shown in Fig. 9; the effects of nucleation are more clearly evident. From the nature of the I–T transients it is clearly seen that the anodic AgI film formation occurs by film growth control and not by a metal dissolution controlled process [15]. Scharifker and Hills [16] have observed the occurrence of nucleation growth process, a common phenomenon in electrodeposition of metals, during anodic film formation of Cu_2S. A similar phenomenon has been observed by us [9] during multilayer formation of AgCl on silver. Thus, the principal rising part of each current transient obtained from 0.01 M KI is a linear function of $T^{1/2}$ (cf. Fig. 10) indicating the instantaneous nucleation–growth processes [17].

However, the current values regress to a positive intercept on the time axis and the intercept is potential dependent (not shown in figure). Non-dimensional plots of I^2/I_m^2 versus T/T_m confirm the formation of AgI on silver by instantaneous nucleation–growth processes.

References

[1] G. J. Moody and J. D. R. Thomas, Selective Ion-sensitive Electrodes, Merrow, Watford (1971).
[2] B. H. Bizsterbosch and J. Lyklema, *Adv. Colloid Interface Sci.* **9** (1978) 147.
[3] Orion Research Analytical Methods Guide, Mass. (1973).
[4] J. Th. G. Overbeek, *J. Colloid Interface Sci.* **58** (1977) 408.
[5] V. I. Birss and G. A. Wright, *Electrochim. Acta* **27** (1982) 1439.
[6] J. P. Karel and H. P. Van Leuven, *J. Electroanal. Chem.* **110** (1980) 119.
[7] K. Kvastek and V. Horvat, *ibid.* **130** (1981) 67.
[8] S. Jaya, T. P. Rao and G. P. Rao, *Bull. Electrochem.*, in press.
[9] *Idem, J. Appl. Electrochem.*, in press.
[10] S. Fletcher, C. S. Halliday, D. Gates, M. Westcott, T. Lwin and G. Nelson, *J. Electroanal. Chem.* **159** (1983) 267.
[11] D. J. G. Ives and G. J. Janz, Reference Electrodes, Academic Press, New York (1961) p. 56.
[12] E. Bosco and S. K. Rangarajan, *J. Electroanal. Chem.* **129** (1981) 25.
[13] H. Angerstein-Kozlowska, J. Klinger and B. E. Conway, *ibid.*, **75** (1977) 45.
[14] E. Laviron, *ibid.*, **101** (1979) 19.
[15] D. A. Varmilyea in 'Advances in Electrochemistry and Electrochemical Engineering', Vol. 3 (edited by P. Delahay), Interscience, New York (1971).
[16] B. Scharifker and G. J. Hills, *Electrochim. Acta* **28** (1983) 879.
[17] G. A. Gunawardena, G. J. Hills, I. Montenegro and B. Scharifker, *J. Electroanal. Chem.* **138** (1982) 225.